Prepared for :
Rijkswaterstaat
Tidal Waters Division
Coastal Genesis Project

Note on parameterisation of long wave effects

A. Reniers
February 1993
DELFT HYDRAULICS
H840.61

Contents

List of Tables

List of Figures

1. Introduction

The cross-shore sediment transport is mainly determined by the time averaged third order odd velocity moment (Ribberink et al,1992).

$$\langle u|u|^2 \rangle$$

This velocity moment can be thought of as a combination of various constituents of which the most important contributions are given by:

$$\langle u|u|^2 \rangle = 3\langle |u_{hi}|^2 \overline{u} \rangle + 3\langle |u_{hi}|^2 u_{lo} \rangle + \langle |u_{hi}|^2 u_{hi} \rangle +$$

Roelvink and Stive (1989) analysed the importance of the various constituents and concluded that short wave asymmetry and the long wave short wave variance interaction term were of the same order of magnitude. They used an empirical approach to obtain this interaction term. This approach is also used in the present version of the cross-shore sediment transport model UNIBEST-TC. It was shown (Saizar, 1990) that this empirical approach can not be applied in general.

A more sophisticated approach to obtain this interaction term is used in the SURFBEAT model (Roelvink,1993). After thorough verification and validation this model has been used to obtain the long-wave short-wave interaction term for a representative bottom profile and a wide range of wave conditions. These results are to be parametrisized to be used in the cross-shore sediment transport model UNIBEST-TC.

2. Environmental conditions

2.1 Bottom profile

The bottom profile used in the computations is based on the 'Bakker'-profile (Roelvink,1993):

$$z_b = z_{b,mean} + A_b \, e^{-\left(\frac{x-x_b}{R_b}\right)^2} \cos 2\pi \left(\frac{x-x_b}{L_b} - \frac{t}{T_b} \right)$$

where:
A_b = maximum bar amplitude
x_b = location of the maximum bar amplitude
R_b = width of the barred profile
l_b = bar length
T_b = typical period of the migrating bar system

The width and location of the bar have been kept constant, which is in correspondence with observed bar behaviour along the Dutch coast.

2.2 Wave conditions

The wave climate is described by the incident wave energy, peak wave period and spectral shape. For the latter a parameterised spectral shape, the JONSWAP spectrum was used, which is described by the root mean square wave height, H_{rms}, peak period, T_p and spectral peakedness parameter γ_p. An additional parameter that has been varied is the bottom friction parameter f_w.

2.3 Variation parameters

The parameters that have been varied are presented in table 2.1., where the asterisk indicates the base value. In the computations only one of the parameters was varied where the other parameters were kept at their base values.

H_{rms} [m]	f_p [1/s]	γ_p	A_b [m]	l_b [m]	t/T_b	f_w
0.25	0.2500	1.0	0.00	100.	0.	0.00
0.50*	0.2222	2.0	0.25	150.	30.	0.01
0.75	0.2000	3.0	0.50	200*	60.	0.02*
1.00*	0.1818	3.3*	0.75	250.	90.	0.03
1.25	0.1667	4.0	1.00*	300.	120.	0.04
1.50	0.1600*	5.0	1.25		150.	0.05
	0.1538	6.0	1.50		180.*	
	0.1428	7.0	1.75			
	0.1333	8.0	2.00			
	0.1250	9.0				
	0.1176	10.0				
	0.1111	12.0				
	0.1053	15.0				
		20.0				

Table 2.1 Variation of parameters

3. Approach

Our interest is in the parameterisation of the long-wave short-wave interaction constituent, which is determined by the correlation between the long wave velocity and variation of the short wave velocities. First an assesment was made of the sensitivity of the correlation coefficient vs. the ratio of actual and incident wave height as function of the various parameters. The results have been presented in Figures 3.1 to 3.7. These show that the correlation is sensitive to a variation in (incident) wave height (Fig. 3.1), peak wave period (Fig. 3.2) and the amplitude of the bar(Fig. 3.4). The latter corresponds to a change in water depth.

With these variables it is possible to generate a number of dimensionless parameters:

$$\frac{H_{rms}}{H_{rms,0}}$$

$$\frac{H_{rms}}{d}$$

$$\frac{gT_p^2}{d_0}$$

Numerous combinations of these parameters were used to obtain a clear relation between the correlation coefficient and the given variables. This process was performed with the MATLAB-program. Some of the results have been presented in Figures 3.8 to 3.10. In general these figures show that there are still significant differences in the correlation coefficients for different incident wave height. These differences increase with increased correlation coefficient. The maximum differences occur near the shore line, where there is a positive correlation due to the standing wave pattern.

The correlation coefficient vs. the ratio of the actual and incident wave energy is presented in Figure 3.10. This shows that there is a difference in correlation coefficient for the various incident wave heights. This is not in correspondence with the results obtained by Roelvink and Stive (1989), who found a linear relation. However, they used the correlation between long-wave surface elevation and wave envelope whereas here the correlation is based on the long wave velocity and short wave velocity variance. The latter is given by:

$$C_r = \frac{cov((u_{hi})^2, u_{lo})}{\sigma_{u_{hi}^2}\sigma_{u_{lo}}}$$

It seems more appropriate to use the root mean square velocity U_{rms} vs. the correlation instead of the root mean square wave height H_{rms}. The near bottom root mean square velocity is given by:

$$U_{rms} = \frac{H_{rms}}{\omega} \frac{1}{\sinh kh}$$

where: k = represents the wave number

Because the wave number is a function of the water depth, U_{rms} is a function of H_{rms} and the water depth. However, the correlation coefficient as function of the squared ratio of actual and incident root mean square velocity, presented in Figure 3.11 proves not to be very useful. Using the near bottom orbital velocity and local water depth vs. the correlation coefficient improves the result, which is presented in Figure 3.12. This shows that there is still a significant difference in correlation coefficients for the various incident wave heights. A similar procedure as described above was used to parameterise the effect of the wave period on the correlation coefficient. One of the results is presented in Figure 3.13. This looks more promising than parameterising the effect of the variation of incident wave height. Near the shoreline, where values of the correlation coefficient become positive, large errors may occur in the parameterisation.

4. Conclusions

These preliminary results indicate that it is not possible to parameterise the correlation coefficient with sufficient accuracy with the variables used. The correlation coefficient is to be used in parameterising other variables corresponding to long waves such as the long-wave short-wave variance interaction term and wave-groupiness. An error in the correlation coefficient yields an additional error in the long-wave short-wave variance interaction term, and thus in the sediment transport.

A possible explanation for this problem is given by the fact that mainly local variables are used in the parameterisation of the correlation coefficient. If there is no information present on what happens at other locations, it is not possible to predict the bound and free long wave amplitudes and thus the correlation coefficient with the required accuracy. As an example we take a location behind the bar with water depth d_x. The root mean square wave height at this location is given by $H_{rms,x}$. If this wave height is a result of (partial) wave breaking on the bar we will find a nearly zero correlation coefficient. This because the wave groups that were present, will have been eliminated by the wave breaking. However, in case of a smaller incident wave height where no wave breaking has occurred, we find a negative correlation coefficient. Including the offshore incident wave height improves the parameterisation results, but without the required accuracy. This indicates that more spatial information on the variables used in the parameterisation is needed.

A different option from parameterisation is to run the SURFBEAT-model for each time step in UNIBEST-TC to compute the long-wave short-wave variance interaction term. However, this will increase the computational effort considerably.

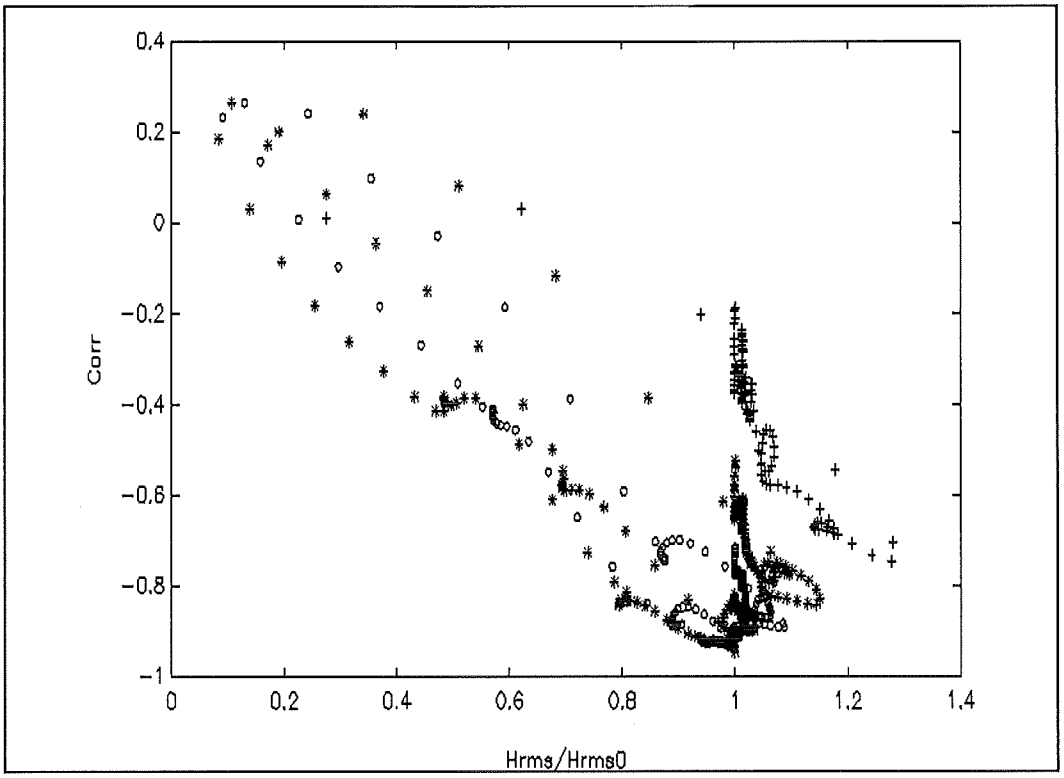

Figure 3.1 Correlation coefficient vs H_{rms}/H_{rms0} as function of H_{rms}

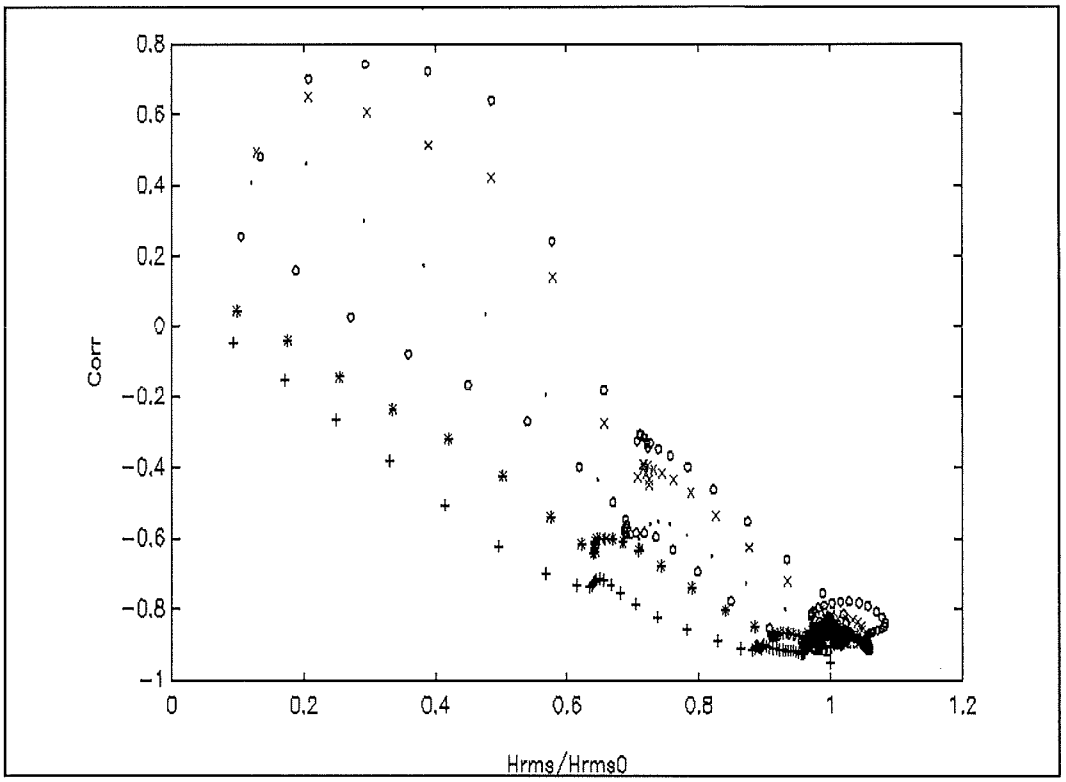

Figure 3.2 Correlation coefficient vs H_{rms}/H_{rms0} as function of f_p

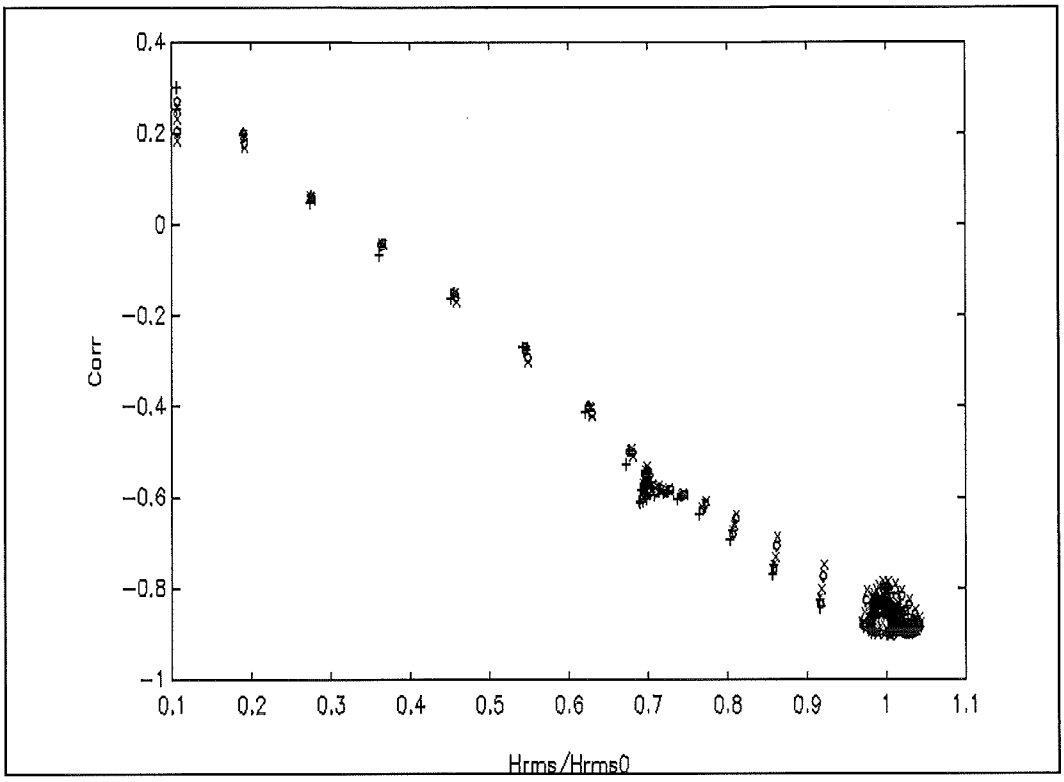

Figure 3.3 Correlation coefficient vs H_{rms}/H_{rms0} as function of γ_p

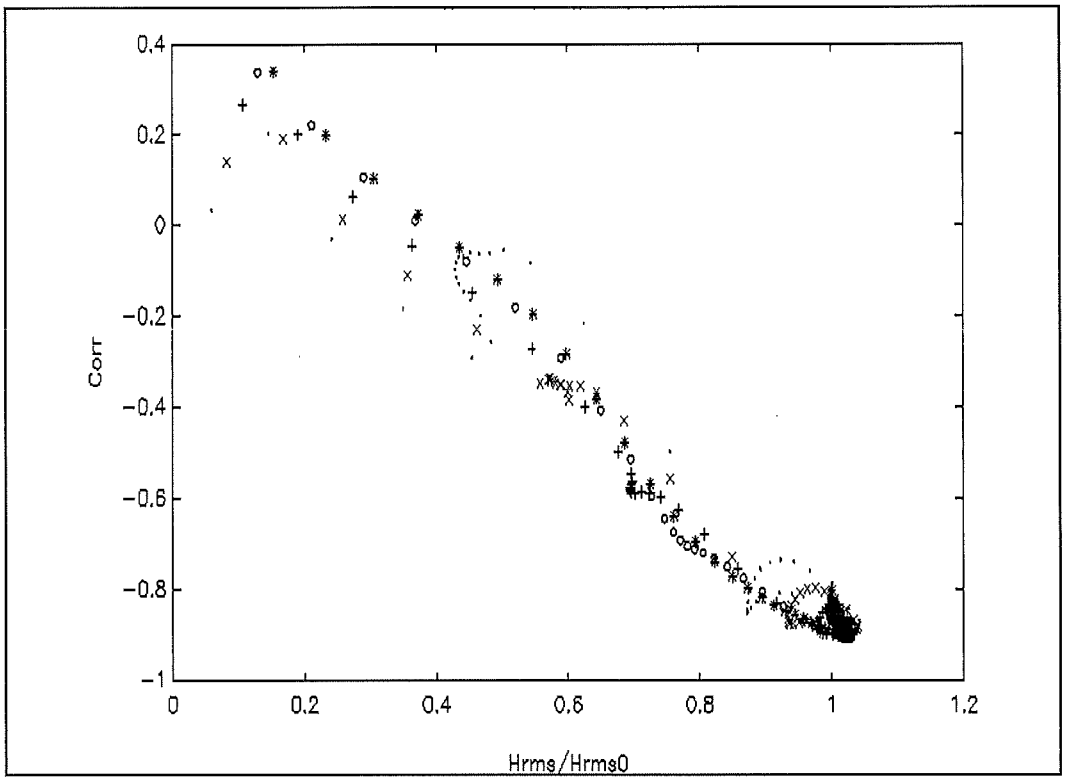

Figure 3.4 Correlation coefficient vs H_{rms}/H_{rms0} as function of A_b

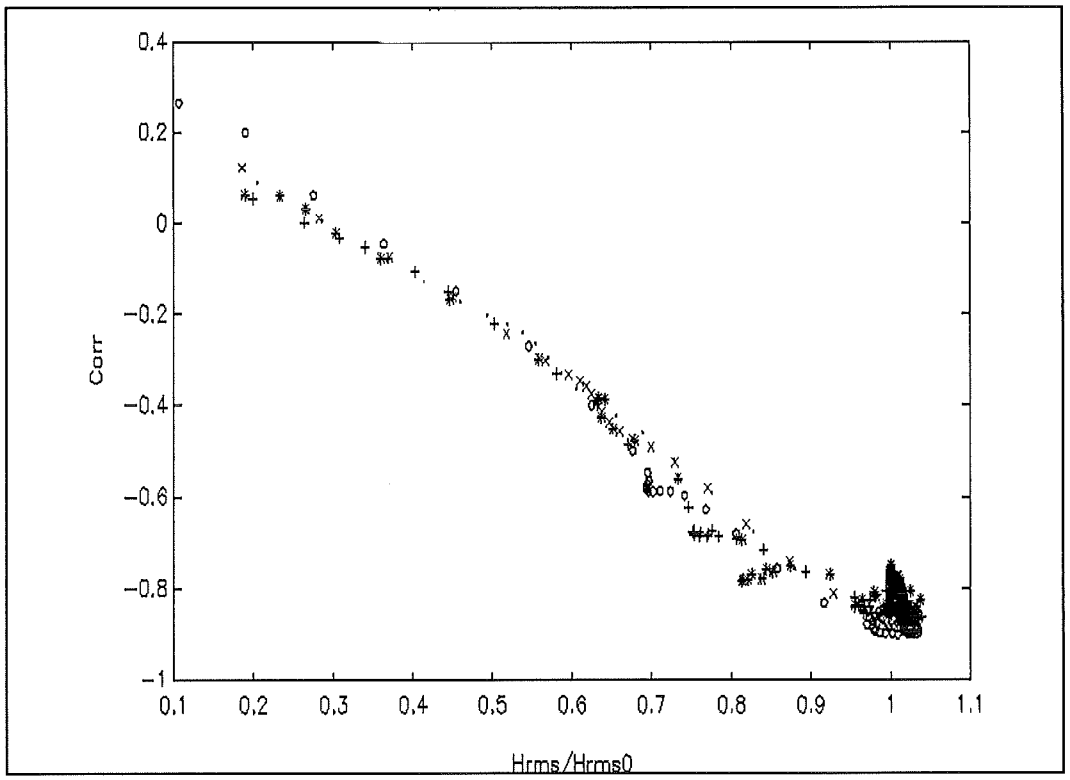

Figure 3.5 Correlation coefficient vs H_{rms}/H_{rms0} as function of L_b

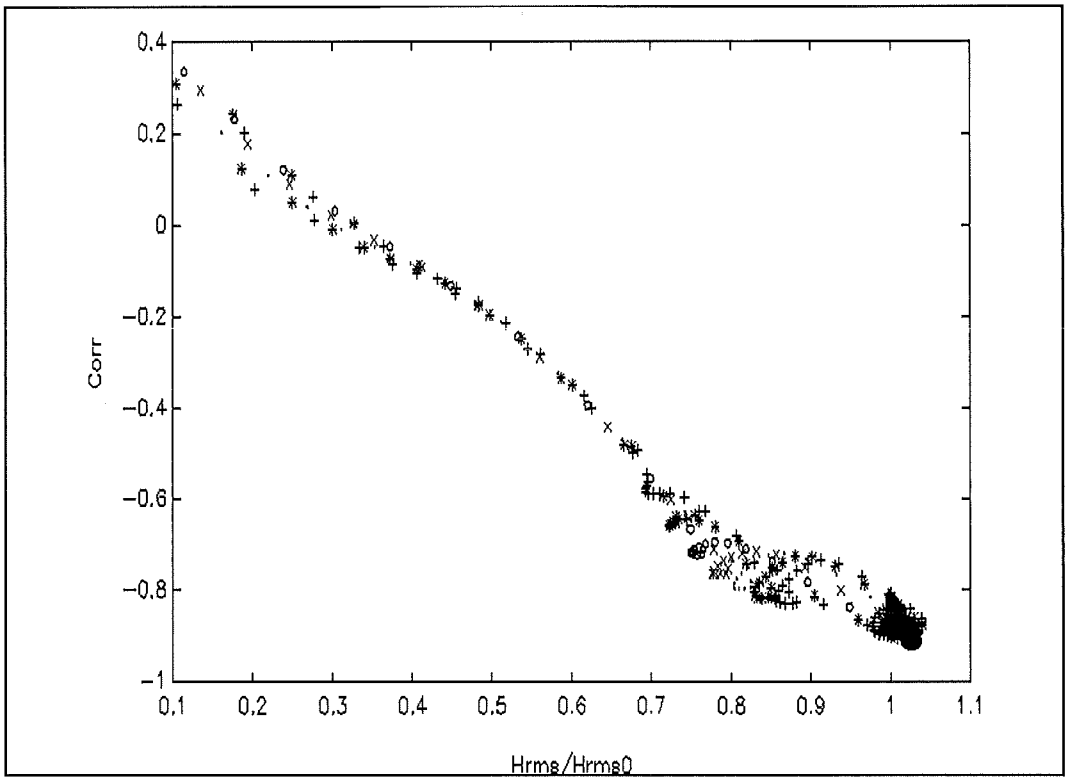

Figure 3.6 Correlation coefficient vs H_{rms}/H_{rms0} as function of t/T_b

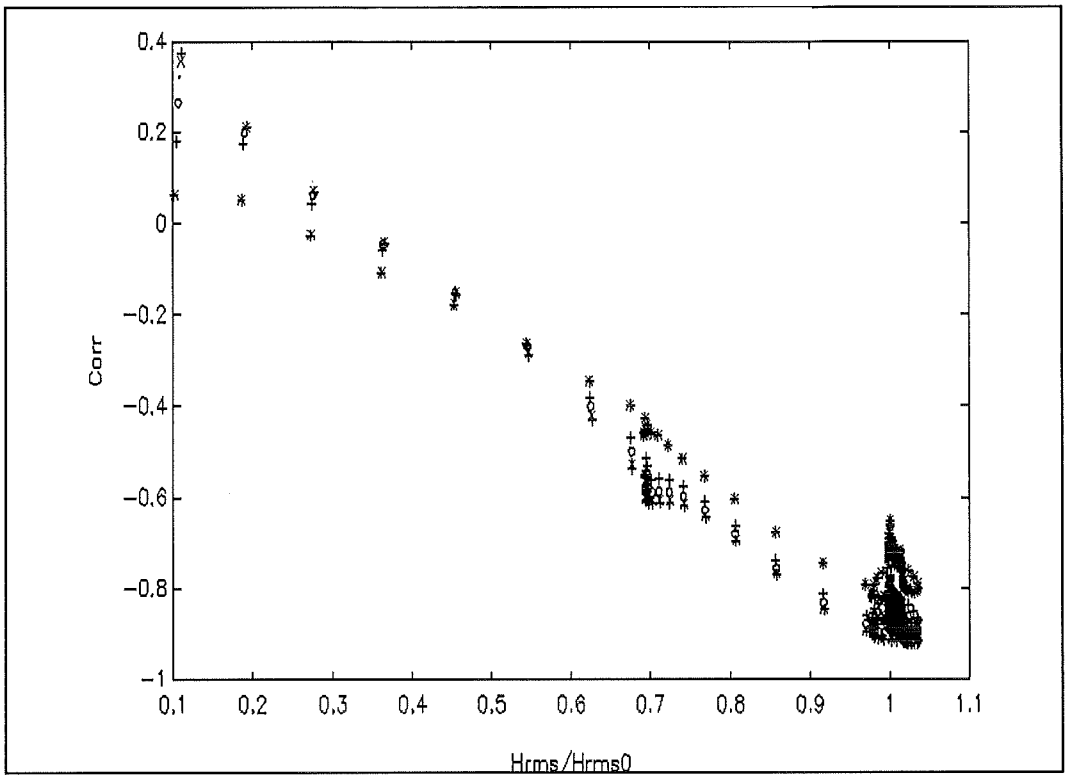

Figure 3.7 Correlation coefficient vs H_{rms}/H_{rms0} as function of f_w

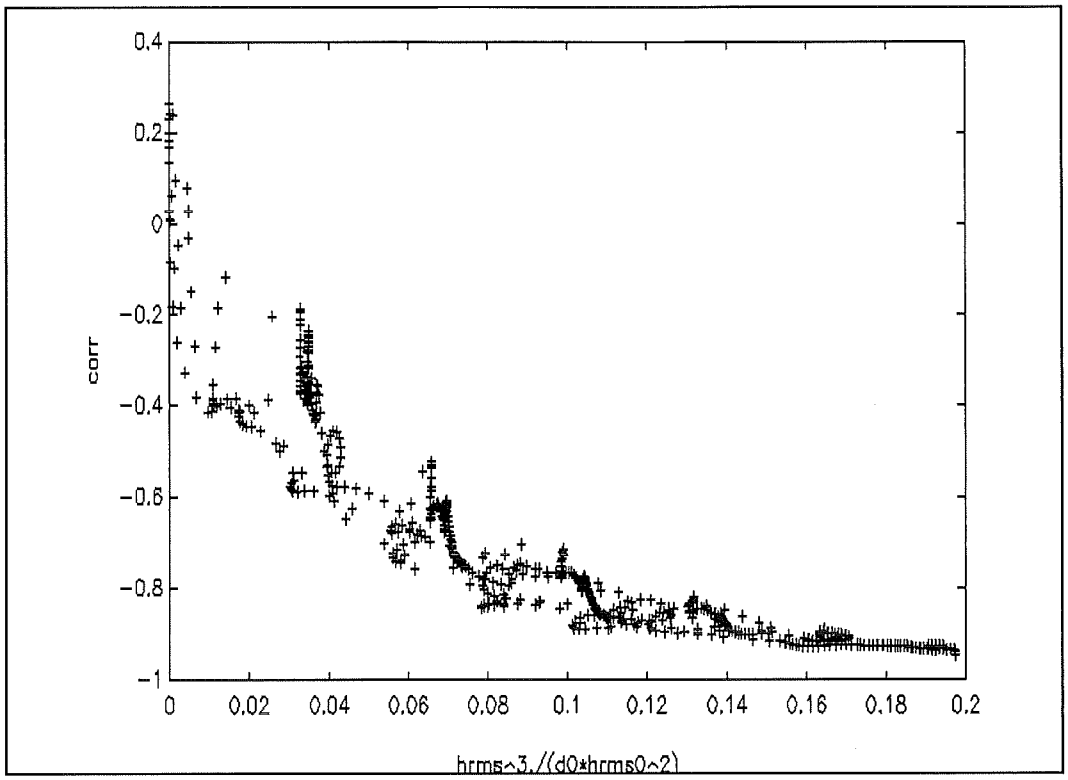

Figure 3.8 Correlation diagram 1, variation of $H_{rms}/H_{rms,0}$

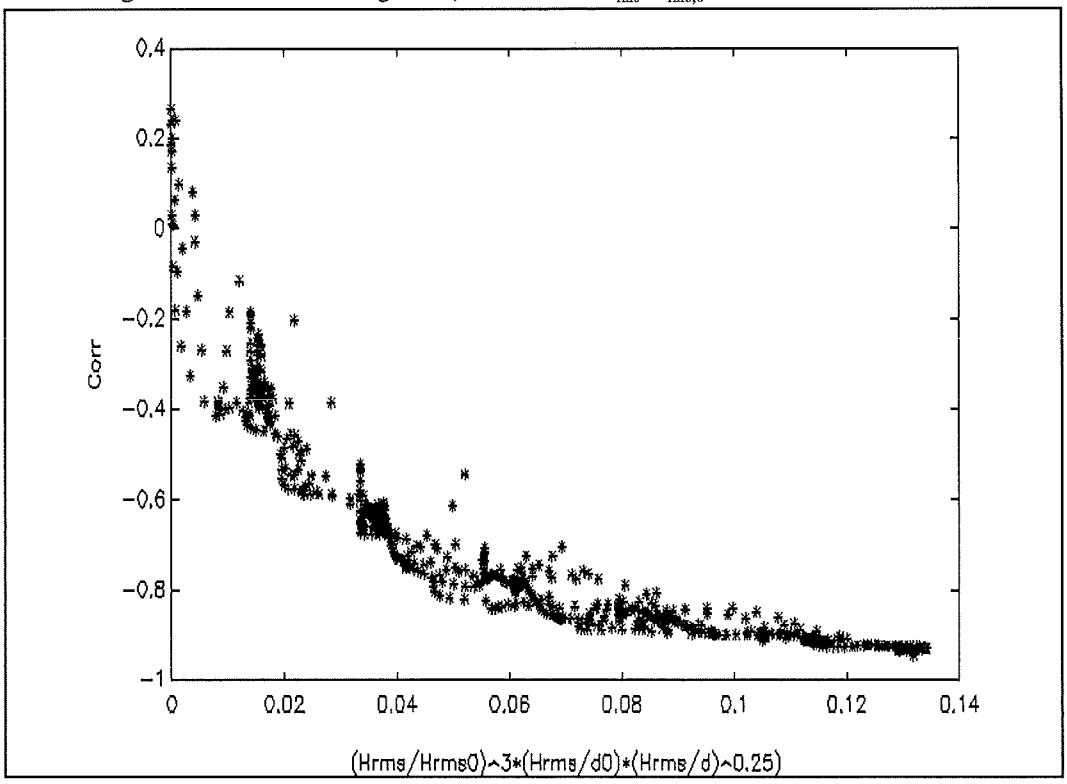

Figure 3.9 Correlation diagram 2, variation of $H_{rms}/H_{rms,0}$

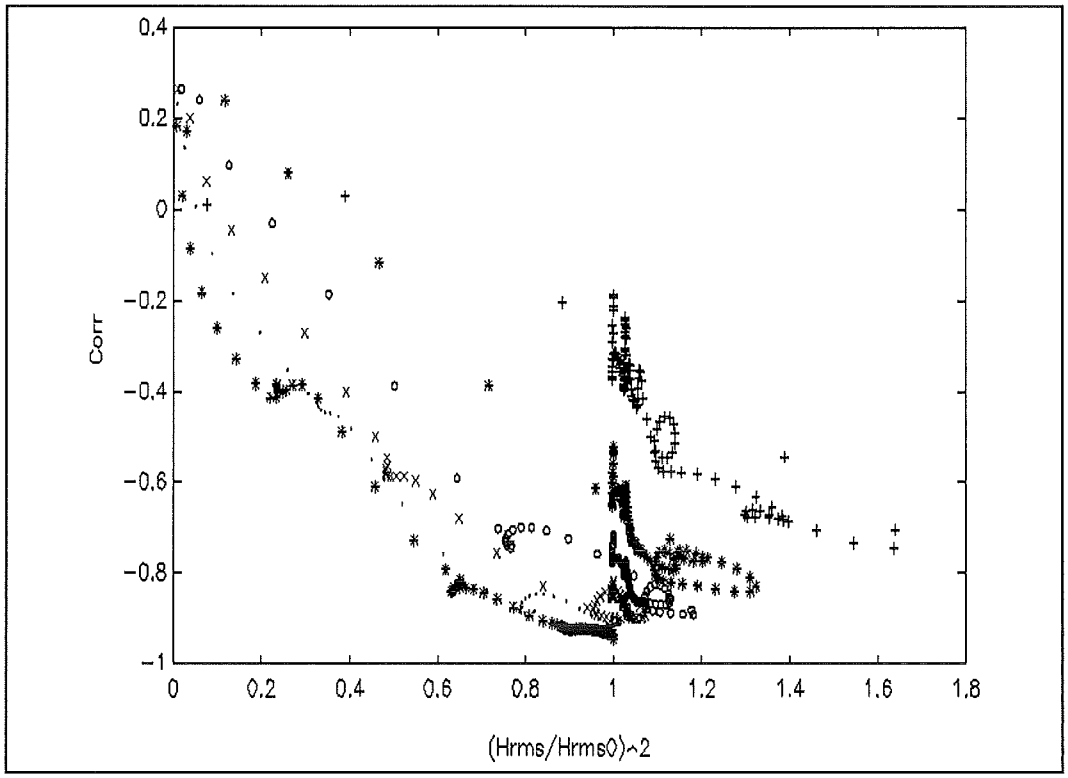

Figure 3.10 Correlation diagram 3, variation of $H_{rms}/H_{rms,0}$

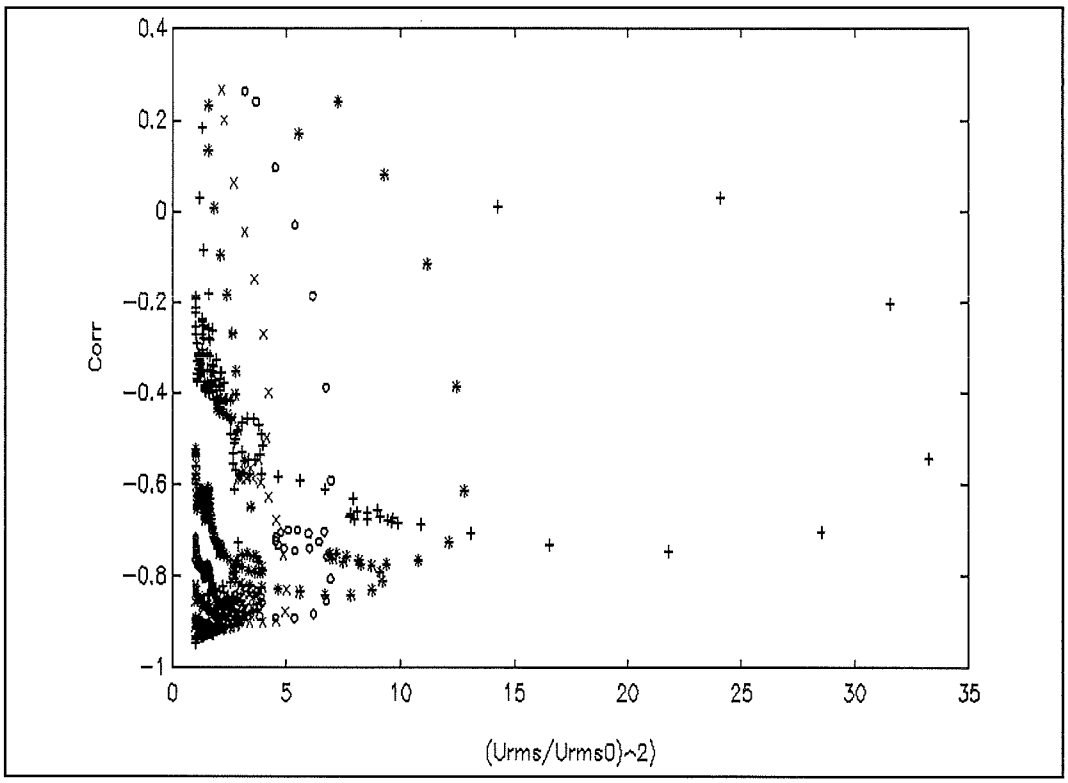

Figure 3.11 Correlation diagram 4, variation of $H_{rms}/H_{rms,0}$

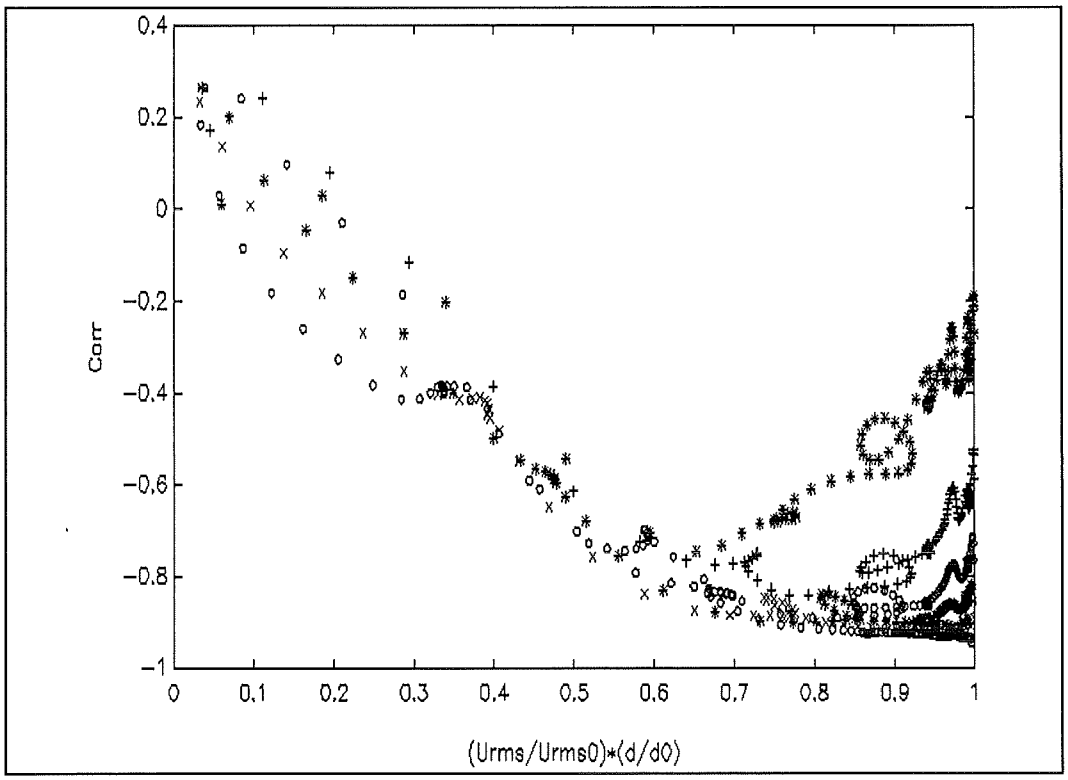

Figure 3.12 Correlation diagram 5, variation of $H_{rms}/H_{rms,0}$

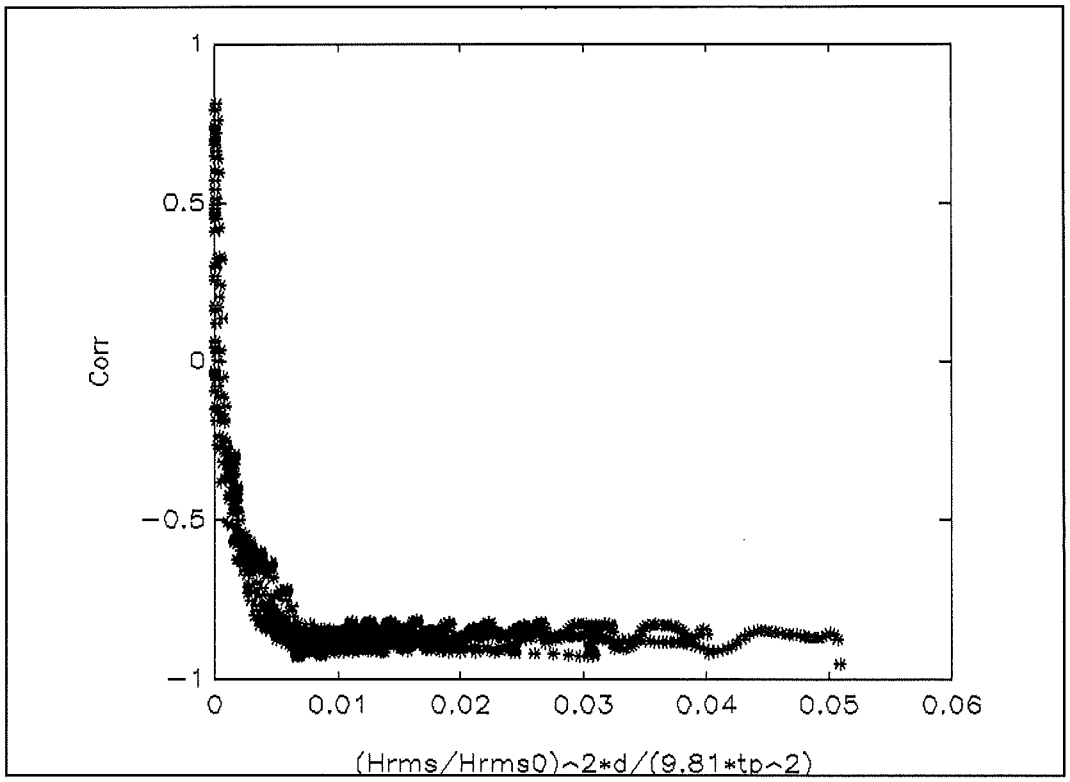

Figure 3.13 Correlation diagram 6, variation of f_p

References

Ribberink, J.S. and A. Al-Salem, 1992:Sediment transports, sediment concentrations and bedforms in simulated asymmetric wave conditions. Experimental study in the large oscillating water tunnel of DELFT HYDRAULICS, Data-report, H 840.20, part V.

Roelvink J.A., 1993:Surf beat and its effect on cross-shore profiles. Ph.D. Thesis (first draft)

Roelvink J.A. and M.J.F. Stive, 1989:Bar-generating cross-shore flow mechanisms on a beach. J. Geophys. Res., vol. 94, no. C4, pp. 4785-4800.

Saizar, A., 1990:The Egmond aan Zee field campaign, November-December 1989, and the use of the data for the validation of a cross-shore sediment transport model. M.Sc. Thesis, Report H.H. 54, IHE Delft.